Journal of Physics: Conference Series **363** (2012) 012004 doi:10.1088/1742-6596/363/1/012004

Newtonian noise and ambient ground motion for gravitational wave detectors

M.G. Beker[1], J.F.J. van den Brand[1,2], E. Hennes[1], D.S. Rabeling[1,2]

[1]National Institute for Subatomic Physics Nikhef, Science Park 105, 1098 XG Amsterdam, The Netherlands

[2]VU University Amsterdam, de Boelelaan 1081, 1081 HV Amsterdam, The Netherlands

E-mail: M.Beker@Nikhef.nl

Abstract. Fluctuations of the local gravitational field as a result of seismic and atmospheric displacements will limit the sensitivity of ground based gravitational wave detectors at frequencies below 10 Hz. We discuss the implications of Newtonian noise for future third generation gravitational wave detectors. The relevant seismic wave fields are predominately of human origin and are dependent on local infrastructure and population density. Seismic studies presented here show that considerable seismic noise reduction is possible compared to current detector locations. A realistic seismic amplitude spectral density of a suitably quiet site should not exceed 0.5 nm/$\sqrt{\text{Hz}}$ (Hz/f)^2 above 1 Hz. Newtonian noise models have been developed both analytically and by finite element analysis. These show that the contribution to Newtonian noise from surface waves due to distance sources significantly reduces with depth. Seismic displacements from local sources and body waves then become the dominant contributors to the Newtonian fluctuations.

1. Introduction

The present interferometric gravitational wave (GW) detectors in the USA (LIGO) and Europe (Virgo) will undergo a major upgrade within the next few years. At the same time KAGRA is being realized in Japan [1]. By 2015 these 'second generation' detectors are expected to come online, with a sensitivity about 10 times better than that of initial designs [2–4]. Increasing the sensitivity of these instruments is a huge experimental endeavor. It will require the suppression of a number of noise sources, including some noise contributors that have previously been considered insignificant. Newtonian noise (NN) is one such noise term that may limit the sensitivity of these advanced detectors in the low frequency band (up to 10 Hz), and is certainly a limiting noise source for 'third generation' detectors that are currently in conceptual design phase.

GW detectors are designed to measure the spatial fluctuations induced by gravitational radiation from astro-physical phenomena. Seismic isolation systems, such as Virgo's super-attenuators [5], have been developed to suppress the mechanical coupling of seismic motion to unwanted vibrations of the interferometer components. However, the resulting transients in the local gravitational field produce Newtonian forces on the interferometer test masses and subsequently inject noise at the interferometer output.

A European project to establish the conceptual design for a third generation GW detector has come to a conclusion this year [6]. The resulting gravitational observatory is coined Einstein

Telescope (ET). ET will improve on the sensitivity of second generation detectors by about another factor of 10 with NN expected to limit performance below 10 Hz. To better understand the problems associated with NN a comprehensive understanding of the expected seismic wave fields is imperative. As part of the ET design study we have conducted a world-wide seismic noise investigation that involved seismic data taking at various sites in Europe and across the globe, as well as the development of analytical and finite element models. Seismic motion in the frequency range of interest predominately originate from human or wind activity. This motivates the choice of third generation detectors, such as ET, to be built underground. Other sources of NN include atmospheric density fluctuations and movement of near-by objects such as people and cars [7]. The latter is a controllable source and atmospheric NN is expected to be less significant than the seismic contribution for underground locations. Here we focus only on seismic NN.

2. Newtonian noise

For a given mass distribution described by a density function $\rho(\mathbf{r},t)$, the acceleration $\mathbf{a}$, experienced by a test mass located at $\mathbf{y}$ is given by

$$\mathbf{a}(\mathbf{y},t) = G\int_V \rho(\mathbf{r},t)\frac{\mathbf{r}'}{|\mathbf{r}'|^3}d^3\mathbf{r}, \quad (1)$$

where $\mathbf{r}' = \mathbf{r}-\mathbf{y}$ and G is the universal gravitational constant. Newtonian noise is associated with density fluctuations of the surrounding geology. When the ground is displaced by a seismic wave field, $\vec{\xi}(\mathbf{r},t)$, density perturbations are produced according to $\delta\rho = -\nabla\rho_0(\mathbf{r})\vec{\xi}(\mathbf{r},t)$. The resulting Newtonian noise term can be written as

$$\delta\mathbf{a}_{NN}(\mathbf{y},t) = G\int_V (\nabla\otimes\frac{\mathbf{r}'}{|\mathbf{r}'|^3})\vec{\xi}(\mathbf{r},t)\rho_0(\mathbf{r})d^3\mathbf{r}, \quad (2)$$

where $\rho_0(\mathbf{r})$ represents the equilibrium density of the medium. The effects of NN on GW detectors have been studied previously [8–10] where the authors present coinciding analytical estimates of NN for surface detectors. Based on these models, it is expected that the sensitivity of Advanced LIGO and Advanced Virgo will be limited around 10 Hz, the lower bound of the detector measurement bandwidth. ET proposes to push the lower bound down to 1.7 Hz, in this way placing more stringent constraints on the level of acceptable seismic noise. To achieve such a broad-band instrument, ET will consist of two separate interferometers, each optimized for respective high and low frequency detections. Fig. 1a shows the projected noise curve for Einstein Telescope's low frequency detector [11]. Newtonian noise is expected to be the major contributor to noise between 2 - 6 Hz. Below 2 Hz it will be limited by ground vibrations coupling mechanically through the conceived seismic isolation systems.

It is important to note that NN is a direct Newtonian coupling between the interferometer test masses and the surrounding geology. It can therefore not be shielded or otherwise mechanically suppressed. In addition it cannot be measured by any instrument other than the interferometer itself. Therefore, finding a suitably quiet seismic environment is the first step in reducing the effects of NN. The level of seismic noise assumed in Fig. 1a is derived from seismic studies and set to 0.5 nm/$\sqrt{\text{Hz}}$ (Hz/f)^2 above 1 Hz. A site with lower seismicity would simply reduce the NN contribution. A reduction by a factor of 3 would, on average be sufficient to let other noise sources, such as suspension thermal and quantum noise dominate. Subtraction techniques are under development [12, 13] that would closely monitor the surrounding geology and predict the resulting NN for each test mass. These predictions can then be subtracted from the interferometer output.

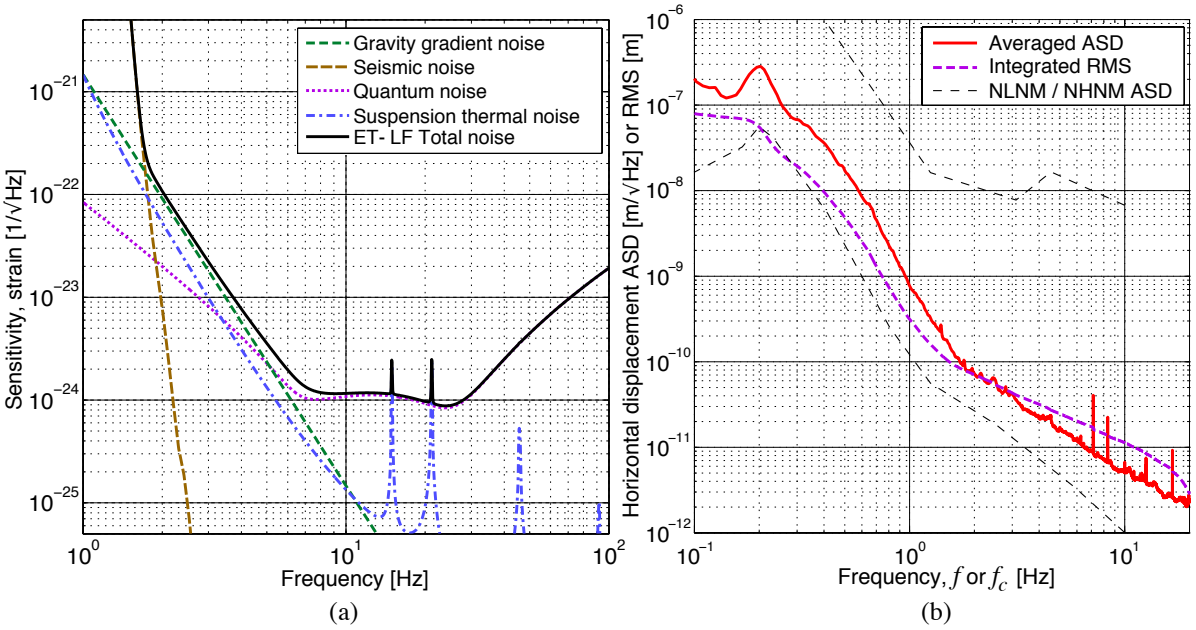

Figure 1. (a) Expected noise budget for ET's low frequency interferometer [11]. Seismic noise (dashed brown curve) will limit sensitivity below 2 Hz and Newtonian noise (dashed green curve) below 6 Hz. (b) A low seismic noise environment as measured at the Canfranc underground laboratory in Spain. The horizontal displacement ASD averaged over several days (red curve) with the corresponding integrated RMS (dashed magenta curve). The dashed black curves represent the Peterson new high and low noise model spectral levels.

3. Ambient ground motion and seismic noise

As part of the ET design project studies were performed to determine seismic noise characteristics at various sites. The studies aim to explore potential locations that yield significant reduction in seismic power spectral density (PSD) in comparison with the current LIGO and Virgo sites, and thus provide a valid estimate of achievable low seismic noise environments in Europe. During the studies the geophysical aspects of underground infrastructure were also considered. Sites were chosen from varying geologies such as clay, salt and hard rock. The study includes 15 locations in 9 European countries, USA and Japan. In the USA two seismometers were installed at the Dusel 3D seismic network [14] in Lead, South Dakota. Data were also taken at the site of KAGRA, the GW detector under construction in the Kamioka mine, Japan. Close collaboration with the Royal Dutch Meteorological Institute [15] provided cross checks of data and analysis techniques at their permanent seismic observatory in The Netherlands. The sites are given in Table 1, with their depth underground, elevation above sea level and indication of general geology, while in Fig. 2 their location is indicated on a map. Two Trillium 240 seismometers were used to obtain seismic data at each site over a period of 1 - 2 weeks, being sure to always include a weekend. All the sites, with the exception of Mol, Belgium, were visited between April 1 and July 30, 2010.

We characterized the sites in terms of RMS displacement and their acceleration power spectral variation. The RMS displacement is the square root of the PSD integrated from the Nyquist frequency to some cut-off frequency, f_c [16]. The horizontal displacement amplitude spectral density (ASD) of the Spanish site and resulting integrated RMS curve are shown in Fig. 1b. The seismic noise levels for all the locations with $f_c = 2$ Hz are given in Table 1. A displacement ASD of 0.5 nm/$\sqrt{\text{Hz}}$ $(\text{Hz}/f)^2$ above 1 Hz, corresponds to an integrated RMS of 0.1 nm (at 2

Location	Depth [m]	Elevation [m]	Seismic noise [nm] (RMS, $f_c = 2$ Hz)	Geology
Spain - LSC, Canfranc	900	1600	0.070	Hard rock
Italy - Sardinia	185	205	0.077†	Hard rock
Hungary - Gyöngyösoroszi	400	400	0.082	Hard rock
	70	400	0.12	
France - LSM, Modane	1750	1000	0.10	Hard rock
Japan - Kamioka	1000	358	0.11	Hard rock
Finland - Sumiainen	0	185	0.11	Surface rock
Italy - Gran Sasso	1400	970	0.13	Hard rock
Germany - Black forest	95	850	0.20	Granite
Romania - Slănic-Prahova	190	195	0.25†	Salt
USA - Dusel, Lead, SD	1250	350	0.64†	Hard rock
	640	960	1.12†	
Germany - Moxa	35	455	0.70	Hard rock
Netherlands - Heimansgroeve	10	135	1.07	Surface rock
Belgium - Mol	230	-205	2.10	Clay
Italy - Sicily	60	-30	9.24†	Salt
Italy - Virgo, Pisa	0	5	54.52	Sedimentary soil

Table 1. Summary of the locations investigated as part of the ET seismic studies. The seismic noise RMS level is obtained from displacement spectra averaged over several days and integrated for frequencies above 2 Hz. A displacement spectrum of 0.5 nm/$\sqrt{\text{Hz}}$ $(\text{Hz}/f)^2$ above 1 Hz, provides a seismic noise RMS of 0.1 nm. For numbers denoted by a dagger (†) mining or other underground activities were underway during data taking.

Hz). The spectral variation is calculated from half hour averaged power spectra. The 90 and 10 percentiles, defined as the level under which the PSD remains for 90 and 10 percent of the time respectively, provide an indication of the variation in the seismic power. A plot of the spectral variation from a selection of sites is given in Fig. 3. The transparent color regions are bounded by the 90 and 10 percentiles while the solid curves are the mode or most common PSD value in each frequency bin. For comparison the spectral variation at the site of the Virgo GW detector is also given. It is clear that selecting a suitable location may improve seismic conditions by several orders of magnitude above 1 Hz.

Results for the Peterson new high (NHNM) and low (NLNM) noise models [17] are also shown in Fig. 3 and Fig. 1b. These models give a theoretical indication of extremely high and low ambient seismic motion respectively. The large peak between 0.1 and 0.3 Hz is known to be generated by oceanic waves. It has been shown that seismic motion from the Dusel array at these frequencies can be correlated with ocean waves from buoy data on the northern Pacific and northern Atlantic [18]. Similarly in Europe, this microseismic peak can be attributed to northern Atlantic ocean activity [19]. Italian sites suffer from an additional analogous peak around 0.5 Hz as a result of Mediterranean sea activity [20].

In the frequency range of interest, seismic activity is dominated by wind and human activity. The seismic wave fields from these sources are excited on, and propagate predominately along the surface, resulting in a reduction in seismic activity with depth [21]. The influence of near-by traffic on GW detectors has been reported before at the LIGO [22] and Virgo [23, 24] sites. This so-called anthropogenic noise is discernible in diurnal patterns in PSD values above 1 Hz, including a clear difference between weekend and weekday spectra. Similar patterns have been attributed to atmospheric effects such as wind. The presence of wind causes movement of surface

Figure 2. Map showing the locations of sites investigated during the ET site studies. Data were collected from the sites indicated by red markers with a dot, whilst third party data were used for the locations represented by blue markers.

objects, such as trees or buildings, or directly through turbulent pressures on topographical irregularities [25, 26]. The day and night ratios for various sites are shown in Fig. 4. There is an obvious dependence on day-time activity except at the Spanish site. This can be explained by the depth and remoteness of the site. It is situated in the northern Pyrenees, where the population density is just 1.38 people per km^2 in comparison with 10, 75 and 180 people per km^2 for the Sardinian, Hungarian and Romania sites respectively. The extreme ratio of the Romanian site is also due to daily mining activities in the same salt structure.

Geophysical aspects of underground construction will play a crucial role in site selection and covers a vast number of topics and considerations. Here we will restrict the discussion to a few general observations. From Table 1 we notice that the most seismically quiet sites are found in hard rock geologies, while the soft geologies such as salt and clay, feature amongst the highest seismic noise environments. In terms of construction of underground facilities, rock stability is a crucial factor, which tends to be more favorable in hard rock geologies. However, subterranean characteristics will also play a role in the transfer of seismic to Newtonian noise as we will demonstrate in the following section.

4. Newtonian noise modeling

Recent studies of NN involve mathematical and finite element (FE) analysis techniques. These attempt to describe NN as a function of depth. A major challenge of underground NN modeling is making correct assumptions about contributions from the various seismic wave types. The wave field in a homogeneous elastic medium can be expressed as a combination of surface and

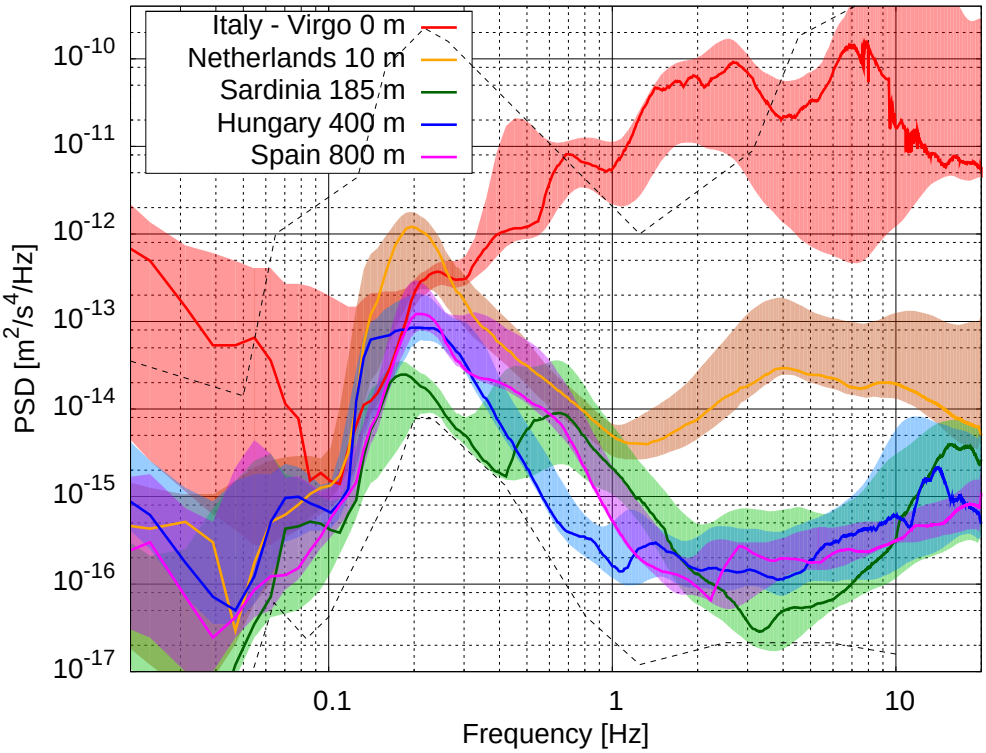

Figure 3. Spectral variation results for various sites. The transparent color regions are bounded by the 90 and 10 percentiles while the solid curves represent the mode or most common PSD value in each frequency bin. The dashed black curves indicate the Peterson new high and low noise models.

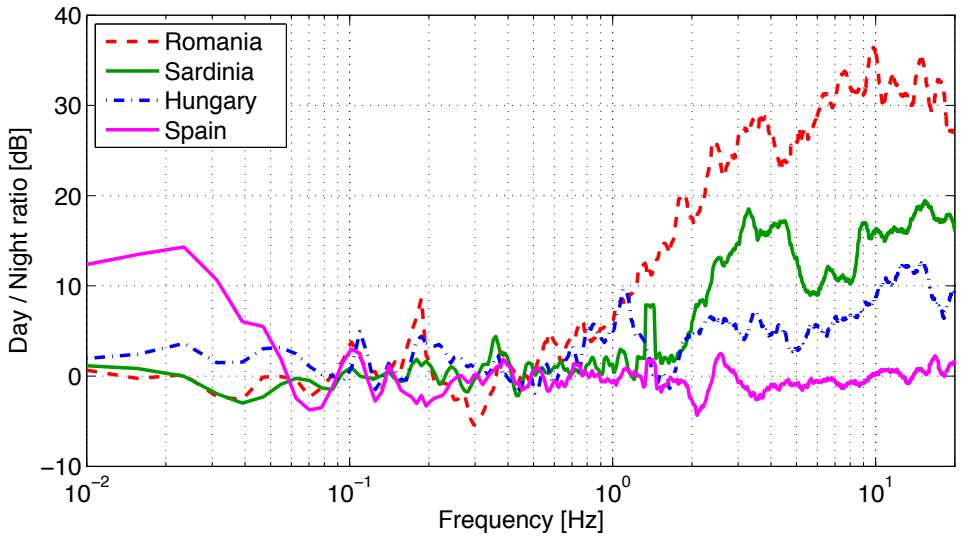

Figure 4. Midday versus midnight noise PSD ratios as a function of frequency. The variations show a strong correlation between seismic noise and human activity at frequencies above 1 Hz. The Romanian site is an extreme case due to the mining activities in the same mine during data taking.

body waves. Two types of body waves exist, pressure (P) and shear (S) waves with respective wave speeds c_P and c_S [27]. In the case of P-waves the movement of a ground particle is parallel to the direction of wave propagation. For S-waves the particle motion is perpendicular to the direction of the wave. In a medium that interfaces with air, two types of surface waves exists: Rayleigh and Love waves. Rayleigh waves produce the largest contribution to NN [9]. They are polarized perpendicular to the surface and vanish with depth.

FE modeling involves subdividing a 3D medium into small volume elements, constituting several corner points called nodes. Within each element the relevant physical parameters, like displacement and stress, are approximated by spline functions that react to a given excitation. The NN calculation is done with the numerical solution to Eq.(2), given by

$$\Delta \mathbf{a}_{NN}(\mathbf{y},t) = G\sum_i (\nabla \otimes \frac{\mathbf{r}_i'}{|\mathbf{r}_i'|^3})\vec{\xi}_i(\mathbf{r},t)m_i, \tag{3}$$

where $m_i = \rho_0 \Delta V_i$ is the mass per node and is assumed constant for all nodes within an element.

Seismic waves can roughly be characterized according to the distance to their source. For near-by or 'local' sources the wave fields are seen to propagate radially away from a single point source. Distant wave fields are excited by sources at a distance, $d \gg \lambda_P = c_P/f$, from the observer. It has been shown that for distant sources an analytical model of the seismic wave field can be constructed from a combination of plane waves [28]. The authors concluded that in such a case the contribution to NN from surface Rayleigh waves is small at depths comparable to the P-wavelength, λ_P. NN will then be dominated by body waves. Note that for hard rock at 1 Hz this involves depths of several kilometers. Similarly FE models have provided predictions for the reduction of NN as a function of depth and wave frequency as shown by the markers in Fig. 5. For comparison results from an analytical model developed by Cella [12, 29] for surface Rayleigh waves are also plotted and show qualitative agreement with the FE results.

For local sources the analytical solutions of the wave fields become more complex and involve all wave field types. In this case we rely on FE analysis, that accurately predicts seismic motion for a given excitation [30]. An example of a FE model displaying a wave field after a local vertical pulse excitation at the origin is shown in Fig. 6a. The model comprises a finite half-space (of which a quarter is shown) of a clay-like medium resulting in a P-wave speed, $c_P = 800$ m/s. The P and S waves can be seen radiating away from the source, with the fastest being the P-wave and the S-wave traveling at roughly half that speed. A Rayleigh wave propagates along the surface at a speed similar to the S-wave. Fig. 6b shows the calculated NN reduction as a function of the depth. The simulations were done along the dashed line shown in Fig. 6a. The reduction in NN as a function of depth is significantly less than expected from the previously discussed distant source Rayleigh wave models. This confirms that NN at depth is dominated by contributions from body waves. These results also clearly reveal the notion that NN suppression with depth increases with lower seismic velocities and higher frequencies.

5. Conclusions

Seismic studies have revealed that future third generation gravitational wave detectors will be able to benefit from significantly lower seismic environments, by up to several orders of magnitude in power spectral density, in comparison with current detector sites. This amounts to a conservative seismic requirement for ET of 0.5 nm/$\sqrt{\text{Hz}}$ (Hz/f)^2 above 1 Hz. At this level NN is expected to limit the interferometer sensitivity from 2 to 6 Hz, with seismic noise being the major contributor below 2 Hz. It is important to note that by simply moving to a more quiet seismic environment both NN and seismic noise will decrease. Subtraction techniques may be used to a posteriori remove part of the NN. Reduction by a factor of 3 will, on average allow suspension thermal and quantum noise to dominate the noise budget at these frequencies.

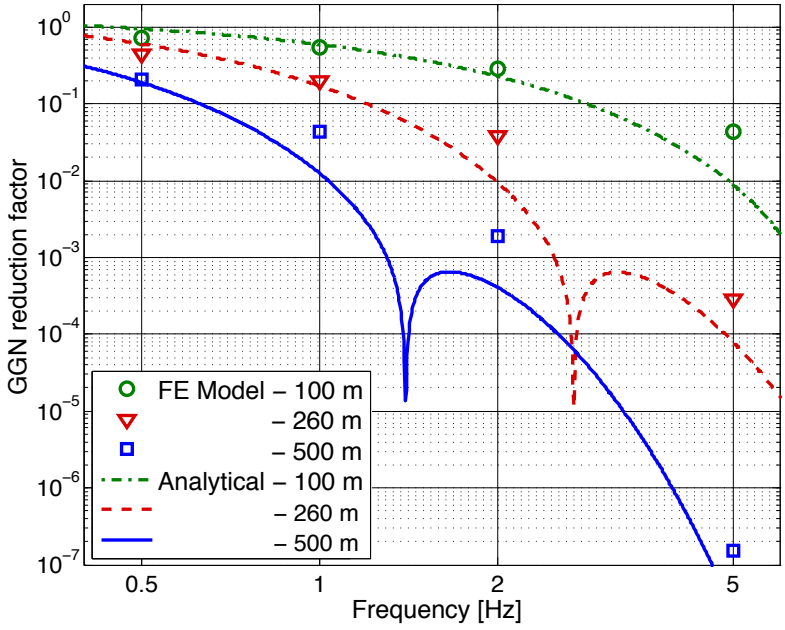

Figure 5. FE simulations of density fluctuations from plane surface waves in a clay-like medium where $c_P = 1000$ m/s. Results show NN reduction compared to surface at 100 (circles), 260 (triangles) and 500 m (squares) depth as a function of frequency. For comparison analytical results from Cella [29] of plane surface Rayleigh waves are indicated by the respective curves.

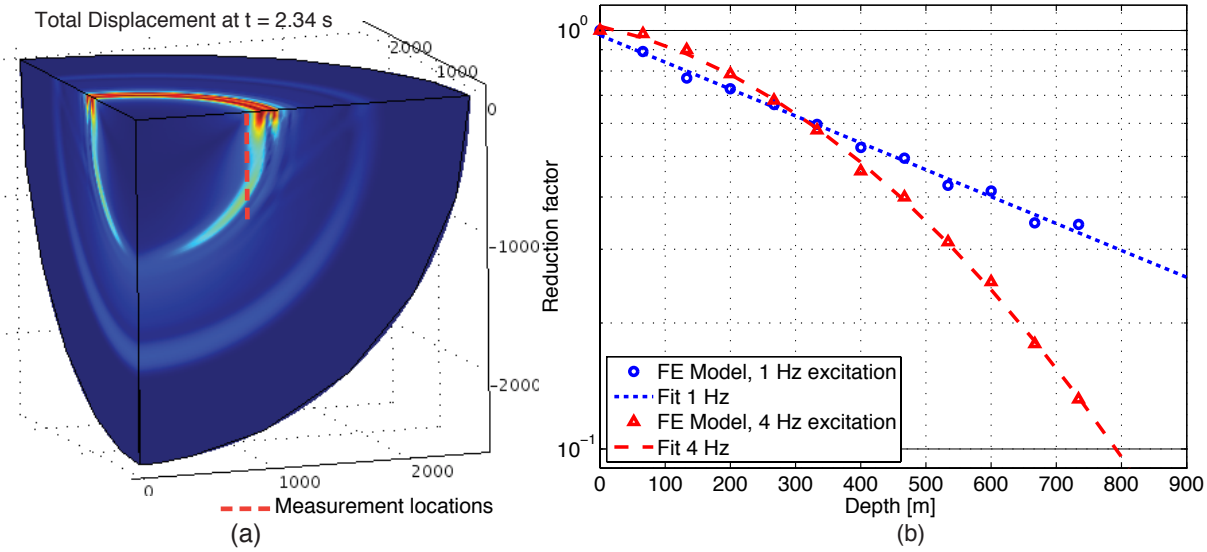

Figure 6. (a) Total displacement for a time domain simulation at 2.34 seconds after a 1 μm vertical pulse excitation at the center of the half-sphere. The P, S and Rayleigh waves can be distinguished. Ground modeled by clay-like medium with a P-wave speed, $c_P = 800$ m/s. (b) NN reduction as a function of depth for 1 and 4 Hz excitations. Simulations done at 800 m (corresponding to λ for 1 Hz waves) horizontally from the excitation point, along the dashed line in (a).

The seismic studies also show that the most quiet sites are in hard rock geologies. While this is unfavorable for NN reduction which is inversely proportional to seismic wave speed, it does provides a stable environment for the construction of large underground facilities. When considering a potential GW detector site, it is important to avoid nearby industry, busy road and train routes and highly populated areas. These anthropogenic sources are the main contributor to seismicity above 1 Hz. Moving underground provides low seismic noise and suppression of atmospheric NN. Additionally, as models have shown, NN contributions from surface waves generated by distant sources significantly attenuate with depth. The remaining NN contributions will then be due to body waves and local seismic sources.

Acknowledgments
We are grateful to many people for their valuable help during seismic data taking, in particular we thank, R. Sleeman, I. Racz, K. Kuroda, F. Ricci, R. Mircea Margineanu, R. Widmer-Schnidrig, J. Harms, R. De Salvo, A. Bettini, M. Zampaolo, E. Coccia and staff at EURIDICE. For discussions on NN we also thank G. Cella. This work has been performed with the support of the European Commission under the Framework Programme 7 (FP7) Capacities, project Einstein Telescope design study (Grant Agreement 211743). This work is part of the research programme of the Foundation for Fundamental Research on Matter (FOM), which is financially supported by the Netherlands Organisation for Scientific Research (NWO).

References
[1] Kuroda K *et al.* 2010 *Class. Quantum Grav.* **27** 084004
[2] Acernese F *et al.* 2008 *Class. Quantum Grav.* **25** 184001
[3] Smith J R for the LIGO Scientific Collaboration 2009 *Class. Quantum Grav.* **26** 114013
[4] Grote H for the LIGO Scientific Collaboration 2010 *Class. Quantum Grav.* **27** 084003
[5] Braccini S *et al.* 2005 *Astroparticle Physics* **23** 557–565
[6] Abernathy M *et al.* 2011 Einstein gravitational wave telescope conceptual design study ET-0106C-10 URL `http://tds.ego-gw.it/`
[7] Thorne K and Winstein C 1999 *Phys. Rev. D* **60** 082001
[8] Saulson P 1984 *Phys. Rev. D* **30** 732–736
[9] Hughes S and Thorne K 1998 *Phys. Rev. D* **58** 122002
[10] Beccaria M *et al.* 1998 *Class. Quantum Grav.* **15** 3339–3362
[11] Hild S *et al.* 2011 *Class. Quantum Grav.* **28** 094013
[12] Beker M *et al.* 2011 *General Relativity and Gravitation* **43** 623–656
[13] Harms J, DeSalvo R, Dorsher S and Mandic V 2009 *arXiv:0910.2774v1 [gr-qc]*
[14] Dusel, Deep Underground Science and Engineering Laboratory URL `http://www.dusel.org`
[15] KNMI, Royal Dutch Meteorological Institute URL `http://www.knmi.nl`
[16] Bialowons W *et al.* 2007 *EUROTeV-Report* **2007-011**
[17] Peterson J 1993 *U.S. Department of Interior Geological Survey* Open-File Report 93-322
[18] Harms J *et al.* 2010 *arXiv:1006.0678v1 [gr-qc]*
[19] A Friedrich F K and Klinge K 1998 *Journal of Seismology* **2** 47–64
[20] Marchetti E and Mazzoni M 2004 *Internal Virgo note* VIR-NOT-FIR-1390-261
[21] Carter J A *et al.* 1991 *Bull. Seism. Soc. of Am.* **81** 1101–1114
[22] Schofield R *et al.* 2000 *LIGO Scientific Collaboration Meeting, Hanford*
[23] Fiori I, Holloway L and Paoletti F 2003 *Internal Virgo Note* VIR-NOT-FIR-1390-251
[24] Acernese F *et al.* 2004 *Class. Quantum Grav.* **21** S433–S440
[25] Withers M *et al.* 1996 *Bull. of the Seism. Soc. of America* **86** 1507–1515
[26] McNamara D E 2004 *Bull. of the Seism. Soc. of America* **94** 1517–1527
[27] Achenbach J 1973 *Wave Propagation in Elastic Solids* (Amsterdam: North-Holland) pp 187–194
[28] Harms J, DeSalvo R, Dorsher S and Mandic V 2009 *Phys. Rev. D* **80**(12) 122001
[29] Cella G 2009 *2nd ET annual workshop, Erice* URL `http://www.et-gw.eu/2ndannualworkshop`
[30] Beker M G, van den Brand J F J, Hennes E and Rabeling D S 2010 *J. Phys.: Conf. Ser.* **228** 012034